Available online at www.sciencedirect.com
SCIENCE DIRECT
Carbohydrate Polymers 59 (2005) 467–475
Carbohydrate Polymers
www.elsevier.com/locate/carbpol

Rheology of starch–clay nanocomposites

Bor-Sen Chiou*, Emma Yee, Greg M. Glenn, William J. Orts

Bioproduct Chemistry and Engineering, Western Regional Research Lab, Agricultural Research Service, United States Department of Agriculture, 800 Buchanan Street, Albany, CA 94710, USA

Received 21 July 2004; revised 26 October 2004; accepted 1 November 2004
Available online 7 December 2004

Abstract

The effects of incorporating various montmorillonite nanoclays into wheat, potato, corn, and waxy corn starch samples were examined by rheology and X-ray diffraction. The nanoclays included the hydrophilic Cloisite Na+ clay as well as the more hydrophobic Cloisite 30B, 10A, and 15A clays. Frequency sweep and creep results for wheat starch–nanoclay samples at room temperature indicated that the Cloisite Na+ samples formed more gel-like materials than the other nanoclay samples. X-ray diffraction results showed no intercalation of Cloisite Na+ clays at room temperature, suggesting that starch granules interacted only with the clay surface and not the interlayer. When the various wheat starch–nanoclay samples were heated to 95 °C, the Cloisite Na+ samples exhibited a large increase in modulus. In contrast, the more hydrophobic nanoclay samples had comparable modulus values to the neat starch sample. These results suggested that during gelatinization, the leached amylose interacted with the Cloisite Na+ interlayer, producing better reinforcement and higher modulus values. X-ray diffraction results supported this interpretation since the data showed greater intercalation of Cloisite Na+ clay in the gelatinized samples. The samples containing wheat and corn starch showed comparable elastic modulus values during gelatinization. However, the potato and waxy corn samples had modulus values that rapidly decreased at higher temperatures.

Keywords: Starch–clay nanocomposites; Nanoclay; Rheology; Gelatinization; X-ray diffraction

1. Introduction

Starch-based materials have emerged as promising alternatives to commodity synthetic polymers because starch is a renewable resource and biodegrades quickly in soil. In contrast, most synthetic polymers are produced from nonrenewable petroleum and do not degrade or degrade very slowly in soil. However, starch-based materials do have some drawbacks. For instance, starch has poor water resistance and relatively poor mechanical properties. Consequently, starch is usually blended with hydrophobic biodegradable polymers to improve the material's water resistance and mechanical properties.

Another method for improving starch properties involves adding nanoclay to starch formulations (McGlashan & Halley, 2003; Park et al., 2002; Park, Lee, Park, Cho, & Ha, 2003). Nanoclays have been previously incorporated into synthetic polymers, resulting in improved barrier, mechanical, and heat resistance properties (Alexandre & Dubois, 2000; Vaia, 2000). The most commonly used nanoclays include montmorillonite, a 2:1 phyllosilicate. Nanoclays have a stacked platelet structure with each platelet having a thickness of approximately 1 nm and lateral dimensions on the order of micrometers. Unmodified nanoclays have a hydrophilic interlayer between each platelet that can be rendered more hydrophobic through a cation exchange process involving alkylammoniums. Park et al. (2003) had shown that incorporating only 5 wt% nanoclay into potato starch reduced water vapor transmission rates by nearly one half. In addition, nanoclay samples exhibited higher dynamic elastic moduli and tensile strengths. The reason for these improvements is that the nanoclays became intercalated, resulting in better dispersed platelets. Consequently, water molecules need to follow a more tortuous path through the composite, leading to lower water vapor transmission rates. In addition, the dispersed platelets provide more surface area for starch–nanoclay interactions,

* Corresponding author. Tel.: +1 510 559 5628; fax: +1 510 559 5675.
E-mail address: bschiou@pw.usda.gov (B.-S. Chiou).

0144-8617/$ - see front matter © 2004 Elsevier Ltd. All rights reserved.
doi:10.1016/j.carbpol.2004.11.001

resulting in better reinforcement and improved mechanical properties.

Up to this point, there have only been a few studies done on starch–clay nanocomposites (McGlashan & Halley, 2003; Park et al., 2002, 2003). Several of these studies involved adding various nanoclays to potato starch (Park et al., 2002, 2003). In addition, a modified nanoclay had been blended with a polyester and a low amylose wheat starch or a high amylose modified maize starch to form blown films (McGlashan & Halley, 2003). These studies have mostly focused on examining the final material properties of the samples. As far as we know, there have been no studies done on measuring the evolving dynamic rheological properties of starch–nanoclay composites during gelatinization. These rheological properties can provide insight into starch–nanoclay interactions as well as material property changes during sample processing.

In addition, only a limited number of studies have examined the dynamic rheological properties of high solids starch formulations (>30 wt% starch) during gelatinization (Chiotelli & Le Meste, 2003; Keetles, van Viliet, & Walstra, 1996; Lii, Shoa, & Tseng, 1995; Rolee & Le Meste, 1997, 1999; Rolee, Chiotelli, & Le Meste, 2002). These concentrated starch formulations have been used when baking starch samples in molds (Glenn, Orts, & Nobes, 2001; Shogren, Lawton, Doane, & Tiefenbacher, 1998) as well as extruding starch products. In fact, dynamic rheological properties measured during heating can provide relevant information on material property changes during starch baking in a mold. The baking process involves low shear, much like the conditions found during a dynamic rheological experiment.

In this study, we examined the dynamic rheological properties of high solids starch–nanoclay formulations containing different types of starches and nanoclays. We varied the nanoclay concentration as well as the moisture content. We first characterized the dynamic moduli and creep behavior of the samples before gelatinization and then measured the evolving dynamic moduli during the gelatinization process. In addition, we used X-ray diffraction to determine the extent of intercalation in the nanoclay samples.

2. Experimental

2.1. Sample formulations

Several different types of starches and nanoclays were examined in this study. The starches included wheat (Midsol 50 from Midwest Grain Products), corn (Melogel), potato (Emsland-Stärke), and waxy corn (Amioca from National Starch). Moisture contents under ambient conditions of these starches were measured by drying them at 150 °C for 20 min in a Mettler Toledo HR73 Halogen Moisture Analyzer. Wheat, corn, potato, and waxy corn starches had moisture contents of 12.5, 11.6, 16.2, and 11.6%, respectively. The different clays were purchased from Southern Clay Products and included Cloisite Na+, Cloisite 30B, Cloisite 10A, and Cloisite 15A, with Na+ being the most hydrophilic and 15A being the most hydrophobic. Cloisite 30B and 10A had intermediate hydrophobicities, with 10A being more hydrophobic than 30B. Cloisite 30B had been modified with methyl, tallow, bis-2-hydroxyethyl, quaternary ammonium, whereas Cloisite 10A had been modified with dimethyl, benzyl, hydrogenated tallow, quaternary ammonium. In addition, Cloisite 15A had been modified with dimethyl, dehydrogenated tallow, quaternary ammonium. The samples were prepared by first adding clays to starch in concentrations of 2.5, 5.0, 7.5, and 10% (w/w) relative to starch. This starch–nanoclay powder was manually mixed in a plastic bag. The moisture contents of samples were then adjusted with deionized water to solid:liquid ratios of 1.5:1 (47% moisture) or 1.25:1 (51% moisture). The moisture contents of each type of starch were taken into account when making the moisture adjustments. Each sample was manually mixed for 5 min. One particular wheat starch sample also contained 15 wt% glycerol (Fisher Scientific) and 36 wt% moisture after adding glycerol as a replacement for one third of the water.

2.2. Rheology experiments

2.2.1. Dynamic tests

Dynamic rheological properties of the starch–clay samples were measured between a 20 mm diameter steel parallel plate and a Peltier plate in an AR2000 rheometer (TA Instruments). The sample was initially mixed and placed on the Peltier plate. The top plate was then lowered to a gap of 1.0 mm from the Peltier plate. To minimize moisture loss during the experiment, the solvent trap on the top plate was filled with deionized water and a thin film of silicone oil (Aldrich) was spread over the outer edge of the sample.

A dynamic rheological test involves applying a sinusoidal strain on the sample and measuring the resulting stress. The applied strain, γ, is (Macosko, 1994)

$$\gamma = \gamma_0 \sin(\omega t) \tag{1}$$

where γ_0 is the strain amplitude, ω is the frequency of oscillation, and t is time. The resulting stress, τ, is then (Macosko, 1994)

$$\tau = G'\gamma_0 \sin(\omega t) + G''\gamma_0 \cos(\omega t) \tag{2}$$

where G' is the elastic modulus and G'' is the viscous modulus. The two moduli characterize the solid (G') and liquid-like (G'') behavior of the material. The elastic modulus measures the elastic response or energy stored per deformation cycle of the material, whereas the viscous

modulus measures the viscous response or the energy dissipated per deformation cycle of the material.

Two different dynamic rheological tests were performed on the samples. One involved measuring the frequency response of the sample at room temperature right after mixing. In this test, the elastic and viscous moduli were measured over a frequency range of 0.04–100 rad/s. The second dynamic rheological test involved monitoring the gelatinization of the starch–clay sample as the sample was heated from 25 to 95 °C at a heating rate of 1 °C/min. The evolving elastic and viscous moduli were monitored at a frequency of 1 rad/s. Both the temperature ramp and frequency sweep experiments were performed within the linear viscoelastic regions of the samples. In addition, all samples were allowed to relax for 15 min prior to the start of each test.

2.2.2. Creep tests

Creep tests were performed using the same parallel plate configuration as the dynamic rheological tests. The sample was sandwiched between the plates at a gap of 1.0 mm. The solvent trap was filled with deionized water and a thin layer of silicone oil was placed around the sample. Stress sweeps were performed on each sample to determine the appropriate applied shear stress used in the creep experiments. In a creep experiment, a constant shear stress is applied to the material and the resulting strain is measured over time. The experimental parameter determined is the creep compliance, $J(t)$, which is defined as (Macosko, 1994)

$$J(t) = \frac{\gamma(t)}{\tau_0} \tag{3}$$

where $\gamma(t)$ is the change in strain as a function of time t and τ_0 is the applied shear stress. The samples in the creep tests were also allowed to relax for 15 min prior to the start of each experiment.

2.3. X-ray diffraction

Nanoclay d_{001} spacings were measured by wide angle X-ray diffraction using a Philips X'Pert MPD X-ray diffractometer. Cu Kα_1 radiation, with a wavelength of 0.154 nm, was used in the experiments and the radiation was generated at 45 kV and 40 mA. The samples were scanned from 1.5 to 60° using a scan speed of 0.1°/s. The d_{001} spacing was calculated by first determining 2θ for the scattering peak using the Phillips X'Pert Data Viewer software and then substituting the 2θ value into Bragg's law.

X-ray diffraction was performed on nanoclay samples before and after gelatinization. The samples before gelatinization were prepared by two methods to determine whether adding water affected the interlayer spacing. The first involved just mixing wheat starch with nanoclay. The second involved adding deionized water to the wheat starch–nanoclay powder and then mixing them together. The sample contained 7.5 wt% clay and had a moisture content of 51%. This sample was allowed to relax 1 h at room temperature before being dried at 40 °C for 24 h. After drying, the caked sample was milled to a powder form using a mortar and pestle. The d_{001} spacings for the two different powders, one without adding water and one processed with water, were then compared using the diffractometer. The samples after gelatinization were prepared in the rheometer using a similar procedure to the rheological tests. The sample was heated from 25 to 95 °C at a rate of 1 °C/min and then cooled back to 25 °C at 5 °C/min. A gap distance of 2 mm between the parallel plates was maintained in the test. The sample contained 5 wt% clay and 51% moisture. After the gelatinization process, the disk-shaped sample was directly placed in the diffractometer for measurements.

3. Results and discussion

3.1. Pre-gelatinization rheology

We first examined the rheological behavior of different nanoclays mixed with wheat starch and water at room temperature and initially focused on samples containing 51% moisture. The samples containing the most hydrophilic nanoclay, Cloisite Na+, exhibited a more gel-like behavior at higher clay concentrations than the other samples. This is shown in Fig. 1, where we plot the elastic modulus of the nanoclay samples as a function of frequency. Except for the 2.5 wt% nanoclay concentration, the Cloisite Na+ samples had the largest elastic modulus values. Moreover, increasing the Cloisite Na+ concentration from 2.5 to 10 wt% resulted in an almost two orders of magnitude increase in the elastic modulus from approximately 3000–200,000 Pa. On the other hand, the more hydrophobic nanoclay samples exhibited an elastic modulus increase of only one order of magnitude over the same concentration range. Also, the Cloisite Na+ samples had an elastic modulus that showed near frequency independent behavior at lower frequencies. This type of behavior indicated a more gel-like material response. In contrast, the other more hydrophobic nanoclays have elastic moduli that showed frequency dependent behavior, especially at low frequencies. This indicated a more liquid-like material response.

Another indication that the Cloisite Na+ samples behaved like a solid or a gel at higher concentrations was the greater difference between their elastic and viscous moduli values. This is shown in Fig. 2, where we plot the elastic and viscous moduli of the 10 wt% nanoclay samples as a function of frequency. The difference between the elastic and viscous moduli values for the Cloisite Na+ sample approached one order of magnitude at the lowest frequencies. In contrast, the other nanoclay samples did not exhibit such a large difference between their moduli values.

We also performed creep experiments on the nanoclay samples to complement the frequency sweeps. The creep

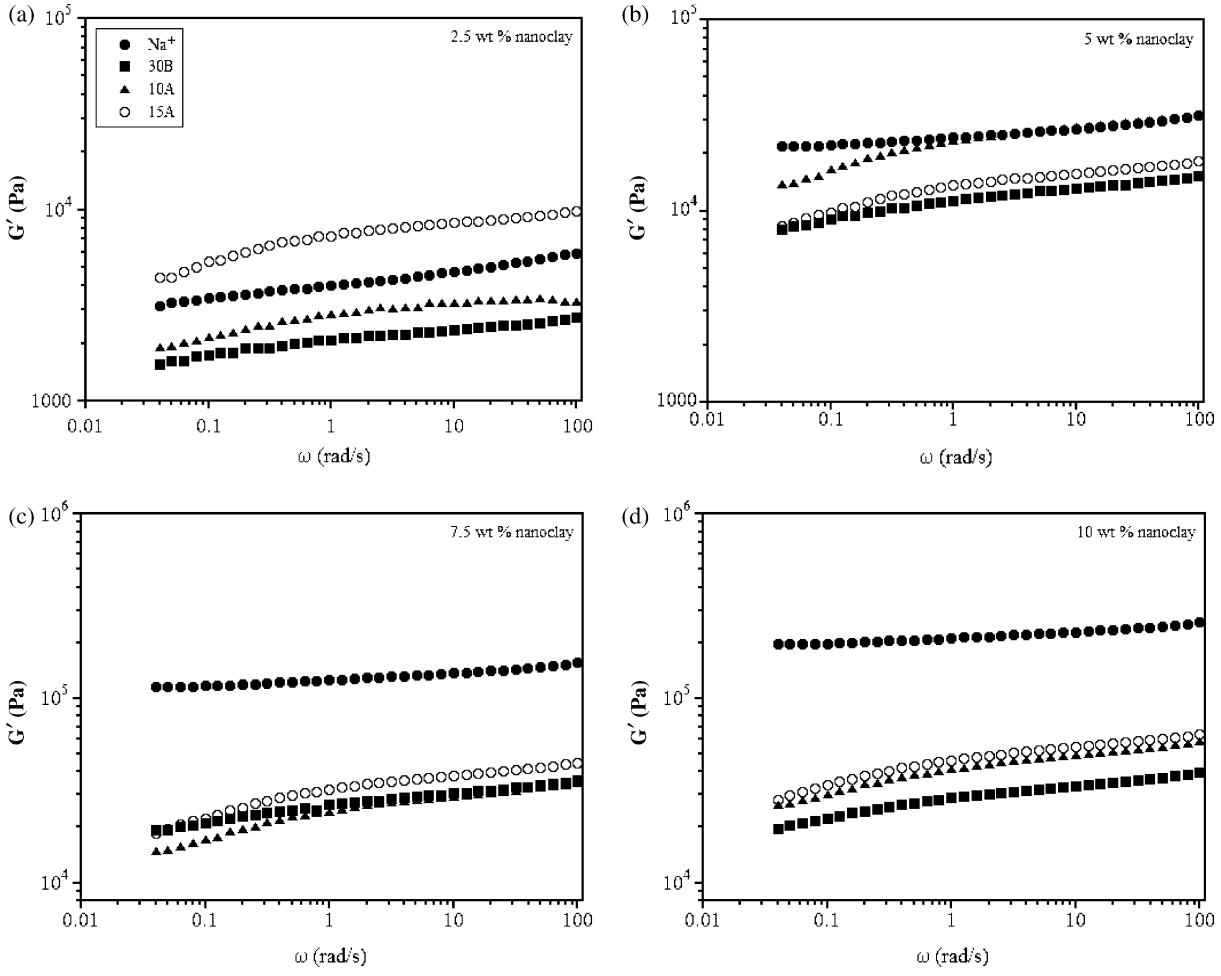

Fig. 1. Elastic moduli of (a) 2.5 wt%, (b) 5.0 wt%, (c) 7.5 wt%, and (d) 10 wt% wheat starch–nanoclay samples as a function of frequency. The moisture content is 51%.

results also indicated that Cloisite Na+ samples had a more solid or gel-like behavior than the other samples. This is shown in Fig. 3, where we plot the creep compliance for the clay samples as a function of time. All samples had a moisture content of 51%. We only present results for the 5 wt% samples because samples at other clay concentrations showed similar creep behavior. The Cloisite Na+ sample had the lowest creep compliance, indicating a more solid-like response, whereas the more hydrophobic nanoclay samples had larger creep compliances, indicating more liquid-like responses. These results are consistent with the frequency sweep data.

Both frequency sweep and creep results indicated that Cloisite Na+ nanoclays had a greater number of interactions with wheat starch than other nanoclays. Such interactions may have produced physical cross-links, leading to Cloisite Na+ samples forming gel-like materials. These interactions only occurred between the granule surface and the nanoclay surface since the starch granules were too large to penetrate into the nanoclay interlayer. Wheat starch granules have a bimodal size distribution, with

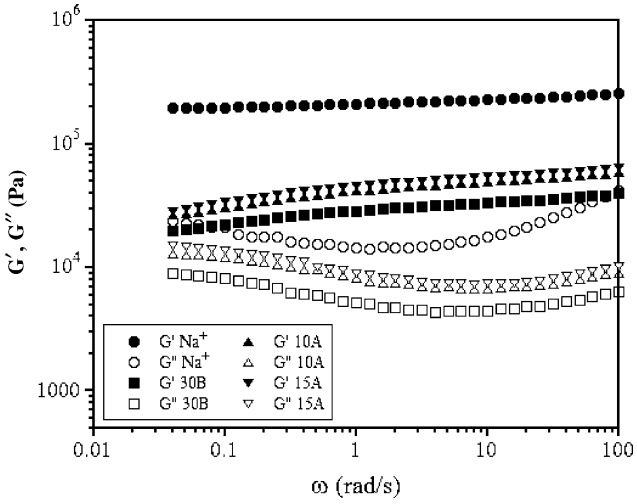

Fig. 2. Elastic and viscous moduli of 10 wt% wheat starch–nanoclay samples as a function of frequency. The moisture content is 51%.

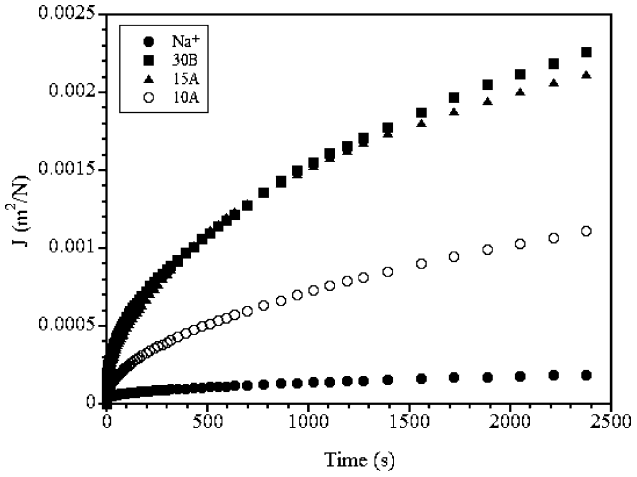

Fig. 3. Creep compliance of 5 wt% wheat starch–nanoclay samples as a function of time. The moisture content is 51%.

smaller granules having dimensions of 2–10 μm and larger granules having dimensions of 20–35 μm (Swinkels, 1985). At room temperature, the granules are insoluble in water and only swell a little bit. X-ray diffraction results showed no intercalation of clay at room temperature after mixing the starch–clay powder with water. This is shown in Fig. 4, where we plot some representative diffraction data for 7.5 wt% Cloisite Na+ and 30B samples. The diffraction peaks for both nanoclay samples did not change after mixing with water, indicating constant interlayer spacings. The Cloisite Na+ had a d_{001} spacing of 1.16 nm, whereas the Cloisite 30B had a d_{001} spacing of 1.87 nm. These spacings are much too small for the starch granules to penetrate into.

Since the Cloisite Na+ nanoclay produced the largest changes on wheat starch rheological properties, we examined the effects of adding it to other starches. We found that wheat and corn starch samples had comparable elastic modulus values, whereas potato and waxy corn

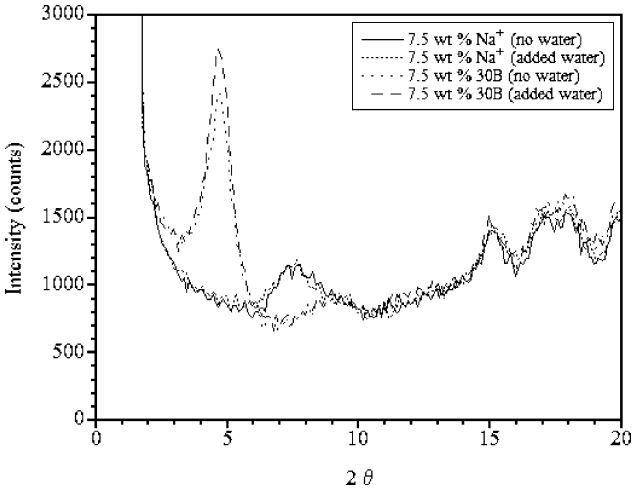

Fig. 4. X-ray diffraction results of 7.5 wt% wheat starch–Cloisite Na+ and 30B samples before and after mixing with deionized water.

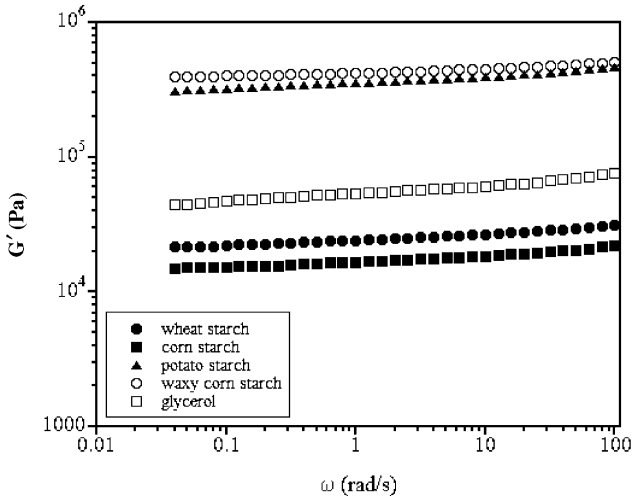

Fig. 5. Elastic moduli of 5 wt% starch–Cloisite Na+ samples as a function of frequency. The moisture content is 51%.

starch samples had much higher elastic modulus values over the nanoclay concentration range. This is shown in Fig. 5, where we plot the elastic modulus of the various starches as a function of frequency. All samples had a moisture content of 51%. We only present results for the 5 wt% samples because the samples for other clay concentrations showed similar trends. All samples had a relatively frequency independent modulus at lower frequencies, indicating they had gel-like structures. Adding glycerol to the wheat starch sample resulted in an increase in the elastic modulus value.

3.2. Rheology during gelatinization

We next examined the evolving elastic modulus of wheat starch–nanoclay samples as they underwent heating from 25 to 95 °C. The Cloisite Na+ samples had a larger elastic modulus than the others at higher temperatures. This is shown in Fig. 6, where we plot the elastic modulus of the different nanoclay samples as a function of temperature. All samples had a moisture content of 51%. The Cloisite Na+ samples had the largest peak modulus values. After the peak temperature, all samples had a modulus that declined in value. However, the Cloisite Na+ samples had modulus values that decreased at a slower rate than the others, resulting in higher modulus values all the way up to 95 °C. In contrast, the more hydrophobic nanoclay samples had comparable modulus values to the neat wheat starch sample after the peak temperature. This indicated that these nanoclays did not have much of a reinforcement effect at elevated temperatures, even though they exhibited a large reinforcement effect at room temperature.

The large increase in the elastic modulus of the Cloisite Na+ samples during heating can be explained by examining the sample's transformation during the heating process. If a starch sample contains sufficient water, the starch gelatinizes as it is heated above a certain temperature. The minimum water content required for wheat starch

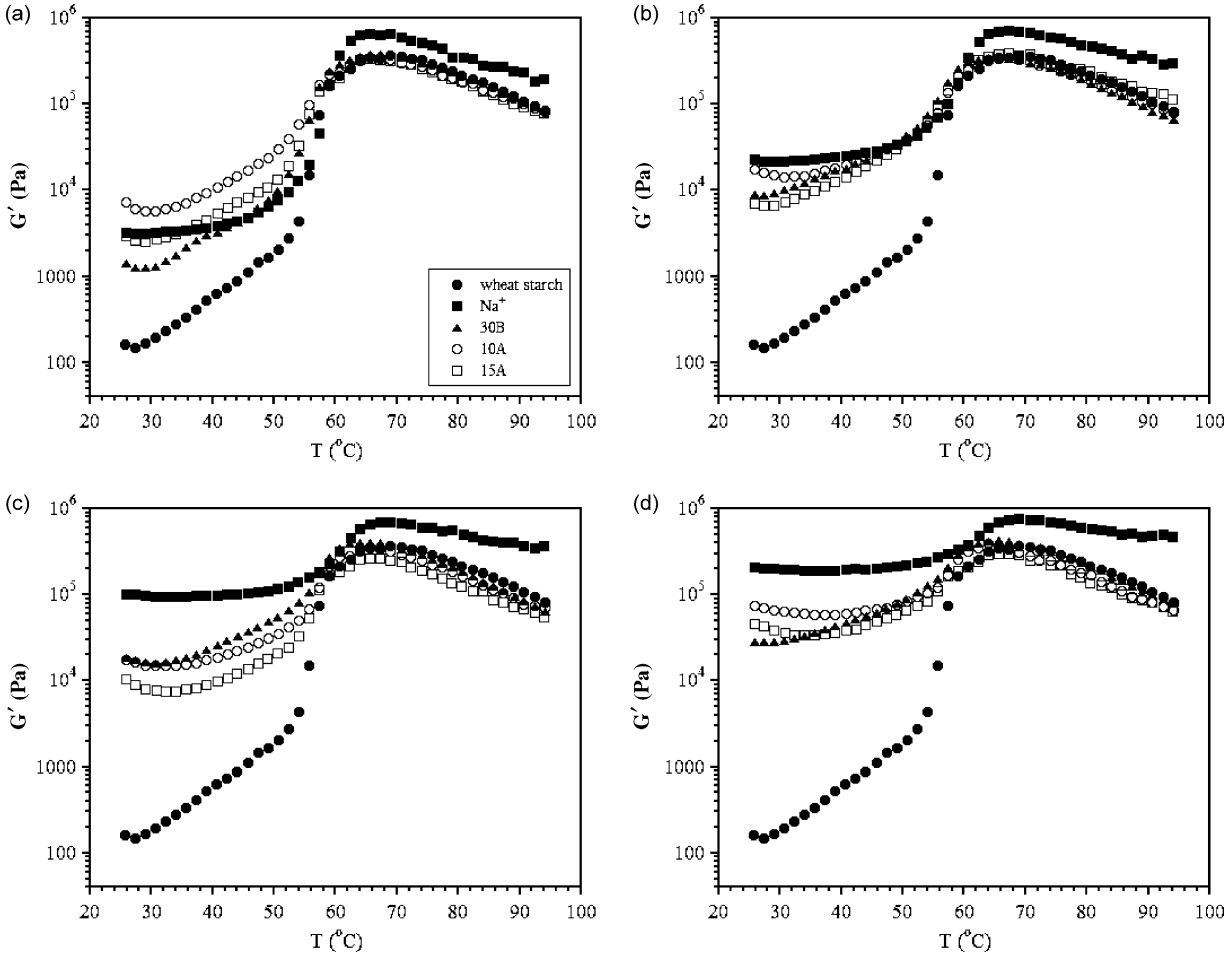

Fig. 6. Evolving elastic moduli of (a) 2.5 wt%, (b) 5.0 wt%, (c) 7.5 wt%, and (d) 10 wt% wheat starch–nanoclay samples as a function of temperature. Neat wheat starch samples are also included in each plot. The moisture content is 51% and the frequency is 1 rad/s.

gelatinization to occur had been determined to be 32–33% (Eliasson, 1980; Wootton & Bamunuarachchi, 1979) from differential scanning calorimetry (DSC). Complete gelatinization only occurs at water contents greater than 65% (Eliasson, 1980; Wootton & Bamunuarachchi, 1979). Nanoclay samples shown in Fig. 6 had a water content of 51%, indicating that only partial gelatinization occurred during the heating process. As the sample is heated, hydrogen bonds in the granules become weakened and the granules begin absorbing more water (Dengate, 1984). This disruption of hydrogen bonds initially occurs in the amorphous region. At around 45–50 °C, the wheat starch granules begin to swell in size (Tester & Morrison, 1990). Mostly amylose leaches out of the granule and becomes solubilized in water. Subsequently, the granules lose their birefringence, as the amylopectin crystallites begin to melt and lose their order. This initial melting of crystallites in various starches, as measured by DSC, has been correlated with the initial increase of the elastic modulus (Kettles et al., 1996; Rolee & Le Meste, 1997, 1999; Tsai, Li, & Lii, 1997). As the crystallites melt and the amylose leaches out, the granules continue to swell in size. The swelling leads to an increase in the granule volume fraction, resulting in a rapid rise in the elastic modulus between 55 and 65 °C. The leached amylose and smaller amount of amylopectin both contain hydroxy groups that can then interact with the hydrophilic Cloisite Na+ nanoclay. The amylose and amylopectin penetrate into the interlayer between the nanoclay platelets and push them further apart. The clay becomes intercalated, resulting in more interactions between clay and starch molecules. The nanoclays then serve as a reinforcement agent, leading to increased modulus values. In contrast, the more hydrophobic nanoclays contain a hydrophobic interlayer, which the amylose and amylopectin cannot readily penetrate into. Consequently, the nanoclay platelets remain stacked, with less surface area available for interaction with starch molecules. This produces less of a reinforcement effect and a lower elastic modulus than the hydrophilic nanoclay (see Fig. 6).

X-ray diffraction results for the nanoclay samples after gelatinization supported the interpretation that starch molecules penetrated the Cloisite Na+ interlayer to a greater extent than the more hydrophobic clay interlayers.

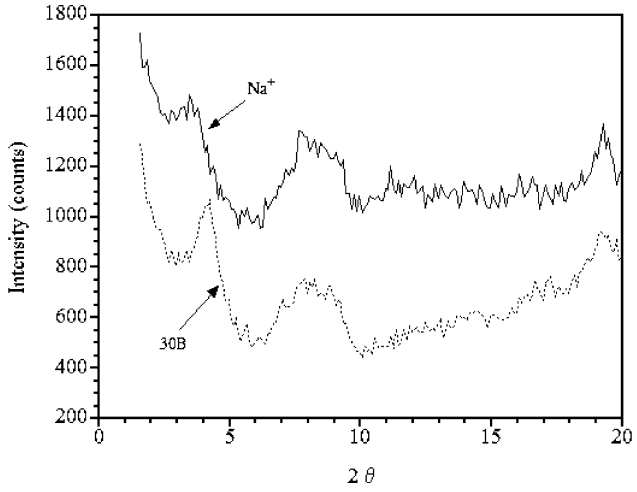

Fig. 7. X-ray diffraction results of 5 wt% Cloisite Na+ and 30B samples after gelatinization. The 5 wt% Cloisite Na+ curve has been shifted up by 200 counts to make the plot clearer.

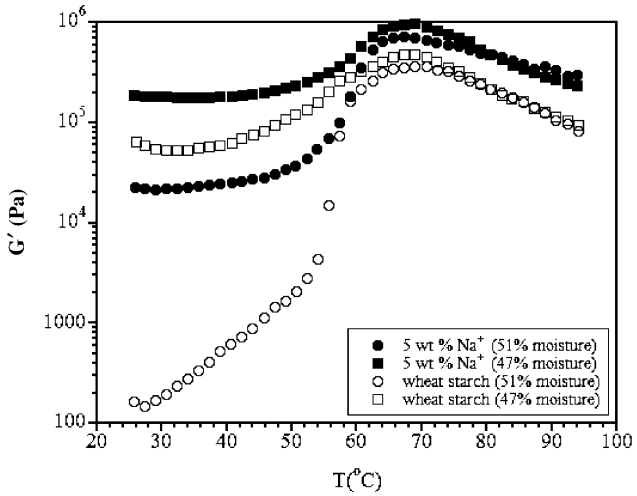

Fig. 8. Evolving elastic moduli of 5 wt% wheat starch–Cloisite Na+ samples and neat wheat starch samples containing different moisture contents as a function of temperature. The frequency is 1 rad/s.

This is shown in Fig. 7, where we plot representative diffraction data for the 5 wt% Cloisite Na+ and 30B samples. The Cloisite Na+ sample had a d_{001} spacing of 2.51 nm, which was greater than the 1.16 nm spacing for pure Cloisite Na+. On the other hand, the Cloisite 30B sample had a d_{001} spacing of 2.11 nm, which was only slightly greater than the 1.87 nm spacing for pure Cloisite 30B. These results suggested that greater intercalation occurred in the Cloisite Na+ sample than the Cloisite 30B sample during gelatinization.

Continued heating of the nanoclay samples eventually led to a decrease in the elastic modulus values. This modulus decrease could be explained by changes occurring in the granule structure. Our nanoclay samples had a high starch concentration and at some point during heating, the swollen granules became closely packed. Further heating of the sample resulted in melting of the remaining crystallites, producing softer granules. This then led to a decrease in modulus. In fact, complete melting of crystallites had been shown to correlate with initial modulus decrease (Keetles et al., 1996). However, the modulus continued to decrease in value even after complete melting had occurred, suggesting that other mechanisms might have contributed to the process. One such mechanism might have involved the granules rupturing at higher temperatures. In addition, it had been suggested that amylopectin chains in the granules might have formed entanglements (Keetles et al., 1996). At higher temperatures, these entanglements could become disrupted, contributing to the modulus decrease.

We next examined the effects of moisture content on the gelatinization behavior of wheat starch–Cloisite Na+ samples. When we decreased the moisture content from 51 to 47%, the lower moisture samples had larger elastic moduli values over most of the temperature range. This is shown in Fig. 8, where we plot the evolving elastic modulus of the 5 wt% Cloisite Na+ samples containing different moisture contents as a function of temperature. Gelatinization curves for the other clay concentrations showed similar trends so we do not present the results here. We also wanted to examine samples containing even lower moisture contents, but those samples became too difficult to produce consistently. Fig. 8 also shows neat wheat starch samples as a comparison. The two neat starch samples had very different modulus values at lower temperatures. However, their modulus values began to converge right after the peak modulus temperature had been reached and became comparable in value thereafter. Similar behavior had been observed for wheat starch samples containing 45 and 50% moisture (Rolee & Le Meste, 1997; Rolee et al., 2002). The nanoclay sample with the lower moisture content had a rather larger modulus than the higher moisture sample and their moduli converged at approximately 78 °C. In addition, the viscous moduli for the nanoclay samples (not shown) also converged at approximately the same temperature. This indicated that the nanoclay samples with different moisture contents had comparable properties after gelatinization.

We also added Cloisite Na+ nanoclay to other starches, including potato, corn, and waxy corn and examined their gelatinization behavior. In addition, we added glycerol to wheat starch and water to produce samples containing 36 wt% moisture and 15 wt% glycerol. Wheat, corn, and glycerol samples exhibited comparable gelatinization behavior, whereas potato and waxy corn samples showed much different behavior. This is shown in Fig. 9, where we plot the elastic modulus of the different starch samples as a function of temperature. We only present results for the 5 wt% nanoclay samples because the samples containing other clay concentrations showed similar behavior. The corn starch curve appeared to be shifted to higher temperatures relative to the wheat starch curve. In fact, the corn starch sample had a peak modulus at approximately 73 °C compared to 66 °C for the wheat starch sample. This higher peak modulus

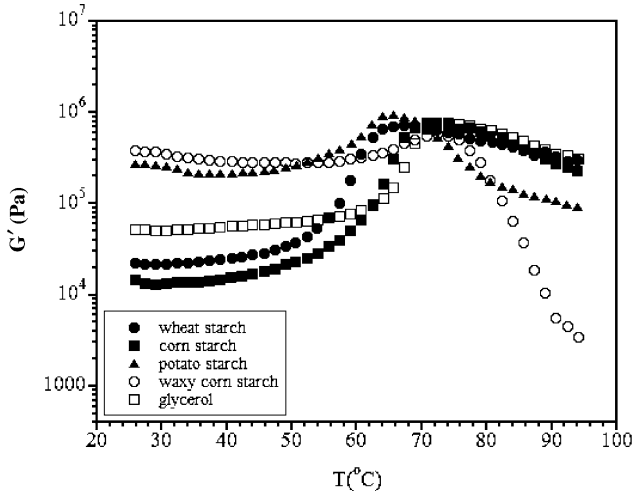

Fig. 9. Evolving moduli of 5 wt% starch–Cloisite Na+ samples as a function of temperature. The moisture content is 51% and the frequency is 1 rad/s.

temperature for corn starch had been observed in several studies (Eliasson, 1986a,b; Singh, Singh, Kaur, Sodhi, & Gill, 2003). One study (Rolee & Le Meste, 1997) did find corn starch having a lower peak modulus temperature. However, the corn and wheat starch samples in that study had different moisture contents. Adding glycerol to wheat starch caused the peak modulus to shift to a higher temperature than that of corn starch. Also, at 95 °C, both the wheat starch and the glycerol samples had a comparable modulus value, which was slightly greater than that of corn starch. The potato starch sample, on the other hand, displayed different gelatinization behavior compared to the wheat, corn, and glycerol samples. Potato starch had a peak modulus at approximately 65 °C, a slightly lower temperature than that of wheat starch. Several studies (Chiotelli & Le Meste, 2003; Keetles et al., 1996; Rolee & Le Meste, 1997; Singh et al., 2003) had shown that potato starch had a peak modulus temperature at around 63–65 °C, which agreed with the results in this study. After the peak temperature, the potato starch modulus dropped rapidly in value. In fact, at the highest temperatures shown in Fig. 9, the potato starch sample had a modulus that was actually lower than the modulus at room temperature. The waxy corn sample also exhibited very different gelatinization behavior than the other starches. The waxy corn modulus peaked at approximately the same temperature as that of corn starch and dropped precipitously after the peak, much like potato starch. However, unlike the other starches, the modulus did not level off, but continued to decline in value until the end of the temperature ramp.

The elastic modulus curves in Fig. 9 for the various starches could be explained in terms of the different physical and chemical properties of each starch and the changes each underwent during gelatinization. Potato and wheat starch samples exhibited an earlier increase in their elastic moduli than corn and waxy corn samples. The initial modulus increase had been correlated with initial crystallite melting. This melting corresponded to the initial gelatinization temperature from DSC measurements. Potato and wheat starches have lower initial gelatinization temperatures than corn and waxy corn starches (Lai & Kokini, 1991; Rolee & Le Meste, 1997; Singh et al., 2003), which is consistent with their earlier modulus rise shown in Fig. 9. The potato starch's low modulus at higher temperatures could be explained by its higher swelling capacity compared to the other starches. This greater swelling capacity could be attributed in part to the higher phosphate concentration located on the amylopectin molecule (Hoover, 2001; Keetles et al., 1996; Singh et al., 2003). Phosphate groups on adjacent amylopectin chains repulse each other, thereby weakening bonds within the crystalline domain. Consequently, hydration becomes easier and potato granules can swell to a larger extent. In addition, corn and wheat starches have higher lipid concentrations than potato starches, which limit their swelling capacity (Dengate, 1984; Hoover, 2001; Singh et al., 2003). Lipids form complexes with amylose, restricting their leaching from granules and consequently, reducing granule swelling. The higher swelling capacity of potato starch ultimately produces softer swollen granules, resulting in lower modulus values at higher temperatures (Keetles et al., 1996). The precipitous drop in waxy corn modulus at high temperatures could be explained by the low amylose concentration present in the granules. For the other starches, amylose leaches out of the granules during gelatinization and can form entanglements with each other or can interact with granule and nanoclay surfaces. The formation of entanglements and physical cross-links produces a sample with a higher elastic modulus. For waxy corn samples, the low amylose concentration precluded such interactions. Consequently, the waxy corn sample had a very low modulus at higher temperatures.

4. Conclusions

Wheat starch granules at room temperature interacted more with the Cloisite Na+ nanoclays than with the other more hydrophobic nanoclays. At higher clay concentrations, the Cloisite Na+ samples had larger, frequency independent elastic moduli and lower creep compliances than the other samples. This indicated that Cloisite Na+ samples formed more gel-like materials. In addition, X-ray diffraction results showed that intercalation did not take place at room temperature, suggesting the platelets remained in a stacked configuration. Consequently, interactions between the starch granule and the nanoclay occurred on the surface and not at the interlayer.

The Cloisite Na+ samples also had larger elastic modulus peaks than the other nanoclay samples during heating and retained larger modulus values up to 95°C. These results suggested that amylose, leached from the granules during gelatinization, interacted more with

the Cloisite Na+ interlayers than with the other clay interlayers. These increased interactions produced greater reinforcement and a higher modulus. X-ray diffraction results supported this interpretation since the data showed greater intercalation of Cloisite Na+ clays. In addition, Cloisite Na+ samples with different moisture contents had comparable dynamic moduli values at 95 °C, indicating similar nanoclay reinforcement properties.

The Cloisite Na+ samples containing wheat and corn starch had comparable elastic modulus values during gelatinization. In contrast, both potato and waxy corn starch samples had elastic modulus values that decreased rapidly at higher temperatures. The potato starch results could be explained in part by potato starch having a higher swelling capacity than other starches. This produced softer granules and led to a lower elastic modulus. On the other hand, the waxy corn starch results could be explained by waxy corn having a very low amylose concentration. The lack of amylose resulted in fewer physical cross-links between leached amylose, starch granule, and nanoclay, leading to a lower elastic modulus.

References

Alexandre, M., & Dubois, P. (2000). Polymer-layered silicate nanocomposites: preparation, properties and uses of a new class of materials. *Materials Science and Engineering*, *28*, 1–63.

Chiotelli, E., & Le Meste, M. (2003). Effect of triglycerides on gelatinisation and rheological properties of concentrated potato starch preparations. *Food Hydrocolloids*, *17*, 629–639.

Dengate, H. N. (1984). Swelling, pasting, and gelling of wheat starch. In Y. Pomeranz (Ed.), *Advances in cereal starch and technology* (pp. 49–82). St Paul, MN: American Association of Cereal Chemists.

Eliasson, A.-C. (1980). Effect of water content on the gelatinization of wheat starch. *Starch*, *32*, 270–272.

Eliasson, A.-C. (1986a). Viscoelastic behavior during the gelatinization of starch I. Comparison of wheat, maize, potato and waxy-barley starches. *Journal of Texture Studies*, *17*, 253–265.

Eliasson, A.-C. (1986b). Viscoelastic behavior during the gelatinization of starch II. Effects of emulsifiers. *Journal of Texture Studies*, *17*, 357–375.

Glenn, G. M., Orts, W. J., & Nobes, G. A. R. (2001). Starch, fiber and $CaCO_3$ effects on the physical properties of foams made by a baking process. *Industrial Crops and Products*, *14*, 201–212.

Hoover, R. (2001). Composition, molecular structure, and physiochemical properties of tuber and root starches: A review. *Carbohydrate Polymers*, *45*, 253–267.

Keetles, C. J. A. M., van Viliet, T., & Walstra, P. (1996). Gelation and retrogradation of concentrated starch systems: 1. Gelation. *Food Hydrocolloids*, *10*, 343–353.

Lai, L. S., & Kokini, J. L. (1991). Physicochemical changes and rheological properties of starch during extrusion (a review). *Biotechnology Progress*, *7*, 251–266.

Lii, C.-Y., Shoa, Y.-Y., & Tseng, K. H. (1995). Gelation mechanism and rheological properties of rice starch. *Carbohydrates*, *72*, 393–400.

Macosko, C. M. (1994). *Rheology principles, measurements, and applications* pp. 109–133. New York: VCH Publishers.

McGlashan, S. A., & Halley, P. J. (2003). Preparation and characterization of biodegradable starch-based nanocomposite materials. *Polymer International*, *52*, 1767–1773.

Park, H.-M., Lee, W.-K., Park, C.-Y., Cho, W.-J., & Ha, C.-S. (2003). Environmentally friendly polymer hybrids Part 1. Mechanical, thermal, and barrier properties of thermoplastic starch/clay nanocomposites. *Journal of Materials Science*, *38*, 909–915.

Park, H.-M., Li, X., Jin, C.-Z., Park, C.-Y., Cho, W.-J., & Ha, C.-S. (2002). Preparation and properties of biodegradable thermoplastic starch/clay hybrids. *Macromolecular Materials and Engineering*, *287*, 553–558.

Rolee, A., Chiotelli, E., & Le Meste, M. (2002). Effect of moisture content on the thermomechanical behavior of concentrated waxy cornstarch–water preparations—A comparison with wheat starch. *Journal of Food Science*, *67*, 1043–1050.

Rolee, A., & Le Meste, M. (1997). Thermomechanical behavior of concentrated starch–water preparations. *Carbohydrates*, *74*, 581–588.

Rolee, A., & Le Meste, M. (1999). Effect of moisture content on thermomechanical behavior of concentrated wheat starch–water preparations. *Cereal Chemistry*, *76*, 452–458.

Shogren, R. L., Lawton, J. W., Doane, W. M., & Tiefenbacher, K. F. (1998). Structure and morphology of baked starch foams. *Polymer*, *39*, 6649–6655.

Singh, N., Singh, J., Kaur, L., Sodhi, N. S., & Gill, B. S. (2003). Morphological, thermal and rheological properties of starches from different botanical sources. *Food Chemistry*, *81*, 219–231.

Swinkels, J. J. M. (1985). Sources of starch, its chemistry and physics. In G. M. A. Van Beynum, & J. A. Roels (Eds.), *Starch conversion technology* (pp. 15–46). New York: Marcel Dekker.

Tester, R. F., & Morrison, W. R. (1990). Swelling and gelatinization of cereal starches. I. Effects of amylopectin, amylose, and lipids. *Cereal Chemistry*, *67*, 551–557.

Tsai, M.-L., Li, C.-F., & Lii, C.-Y. (1997). Effects of granular structures on the pasting behaviors of starches. *Carbohydrates*, *74*, 750–757.

Vaia, R. A. (2000). In T. J. Pinnavaia, & G. W. Beall (Eds.), *Polymer–clay nanocomposites* (pp. 229–266). New York: Wiley.

Wootton, M., & Bamunuarachchi, A. (1979). Application of differential scanning calorimetry to starch gelatinization. *Starch*, *31*, 262–264.